Influence of the Content and Environment of Chromium in CrSiBEA Zeolites on the Oxidative Dehydrogenation of Propane

Janusz Janas,[†] Jacek Gurgul,[†] Robert P. Socha,[†] Jolanta Kowalska,[‡] Krystyna Nowinska,*[,‡] Tetsuya Shishido,[§] Michel Che,[||,⊥,#] and Stanislaw Dzwigaj*[,||,⊥]

Institute of Catalysis and Surface Chemistry, Polish Academy of Sciences, ul. Niezapominajek 8, 30-239 Kraków, Poland, Department of Chemistry, A. Mickiewicz University, Grunwaldzka 6, 60-780 Poznan, Poland, Department of Molecular Engineering, Kyoto University, Kyoto, 615-8510, Japan, UPMC Université Paris 6, UMR 7197, Laboratoire de Réactivité de Surface, 4 Place Jussieu, 75252 Paris Cedex 05, France, and CNRS, UMR 7197, Laboratoire de Réactivité de Surface, 4 Place Jussieu, 75252 Paris Cedex 05, France, Institut Universitaire de France, 103, Boulevard Saint-Michel, 75005, Paris

Received: November 4, 2008; Revised Manuscript Received: June 6, 2009

Cr_xSiBEA catalysts ($x = 0.2$, 1.0, and 3.4 Cr wt %) are prepared by a two-step postsynthesis method. The introduction of Cr ions in the framework of dealuminated SiBEA zeolite evidenced by XRD generates Brønsted acidic sites as shown by FTIR of pyridine used as molecular probe. In Cr_xSiBEA as prepared, chromium is mainly present as octahedral Cr(III) and in calcined Cr_xSiBEA (773 K, 3 h, flowing air) as distorted tetrahedral Cr(VI), as evidenced by DR UV−vis, TPR, and XPS. Upon outgassing of calcined Cr_xSiBEA at 773 K for 1 h (10^{-3} Pa), part of Cr(VI) is reduced to distorted tetrahedral Cr(V), as shown by EPR. Isolated distorted tetrahedral Cr sites present in activated Cr_xSiBEA are responsible for their catalytic activity in the oxidative dehydrogenation (ODH) of propane, performed in the presence of air or N_2O. The propane conversion increases with Cr content in the presence of air or N_2O, while the selectivity toward propene depends on the reaction temperature and oxidant. In the presence of air, the selectivity toward propene is highest for 1.0 Cr wt %. The lower selectivity for the content of 3.4 Cr wt % may be the result of the presence of some amount of extra-framework octahedral Cr sites. The lower propane conversion and the higher selectivity toward propene in the presence of N_2O probably depend on the oxidation state of Cr under reaction conditions and on the nature of surface oxygen. The presence of isolated tetrahedral chromium sites with oxidation state lower than (VI) on activated Cr_xSiBEA is essential for maintaining a high selectivity.

Introduction

Important efforts have been made to develop active and selective catalysts for the oxidative dehydrogenation (ODH) of light alkanes to the corresponding alkenes.[1−8] Microporous materials with isolated tetrahedral V(V) have been found to be active and selective catalysts.[4,5,8−12] However, vanadium oligomers have also been proposed,[13] and the nature and environment of the V sites involved are still a matter of discussion.[14]

Catalysis data on ODH of light alkanes[11,12,14−16] suggest that the presence of isolated mononuclear V and Cr ions is a key factor. The reducibility and acid−base properties of the active sites are also important factors which can influence the rate of alkane conversion and desorption of the reaction intermediate.[6,14,17]

N_2O has recently been used as oxidant for ODH, particularly on Fe and Co-containing ZSM-5.[18−20] Other zeolites, such as BEA, mordenite, and faujasite, modified with Fe[18] and Co[20] have been also used. BEA and ZSM-5 zeolites show comparable activity for ODH of propane, while mordenite and faujasite are much less active and mainly lead to CO_x.[18]

Since framework transition metal ions are considered to be active in selective oxidation reactions[21−24] and the amount introduced by direct hydrothermal synthesis is usually low,[25,26] a two-step postsynthesis method was developed.[27] It consists first in the removal of Al from BEA zeolite by treatment with nitric acid, followed by the introduction of V by impregnating the resulting SiBEA with NH_4VO_3 aqueous solution. This method allows incorporation of isolated tetrahedral V(V),[27−29] Co(II),[30−32] or Fe(III)[32,33] into BEA zeolite with low metal content (to 2 wt %).

In this work, Cr_xSiBEA zeolites obtained by this method are characterized by XRD, FTIR, DR UV−vis, TPR, XPS, and EPR, and the influence of the content and environment of chromium on their catalytic activity in ODH of propane with air or N_2O is investigated.

Experimental Section

Catalyst Preparation. Cr_xSiBEA catalysts ($x = 0.2$, 1.0, and 3.4 Cr wt %) were prepared by the two-step postsynthesis method reported earlier.[27−29] Two grams of siliceous BEA zeolite (Si/Al > 1300), referred to as SiBEA, obtained by treatment of a tetraethylammonium BEA zeolite (Si/Al = 11, crystal size around 0.5 μm in diameter, surface area of 660 $m^2\ g^{-1}$, micropore volume of 0.25 $cm^3\ g^{-1}$) with a 13 mol L^{-1} HNO_3 solution (4 h, 353 K), was stirred for 24 h at 298 K in aqueous solutions containing from 0.8×10^{-3} to 15.2×10^{-3} mol L^{-1} of $Cr(NO_3)_3 \cdot 9H_2O$. Then, the suspension (pH 2.6) was stirred for 2 h in air at 353 K until complete evaporation of

* To whom correspondence should be addressed. E-mail: krysnow@amu.edu.pl (K.N.); stanislaw.dzwigaj@upmc.fr (S.D.).
† Polish Academy of Sciences.
‡ A. Mickiewicz University.
§ Kyoto University.
|| UPMC Université Paris 6.
⊥ CNRS.
Institut Universitaire de France.

10.1021/jp809733s CCC: $40.75
Published on Web 07/01/2009

water. The resulting solids, dried in air at 353 K for 24 h and containing of 0.2, 1.0, and 3.4 Cr wt %, were labeled $Cr_{0.2}$SiBEA, $Cr_{1.0}$SiBEA, and $Cr_{3.4}$SiBEA, respectively. All samples were light-green with color intensity increasing with the Cr content. Prior to characterization, Cr_xSiBEA samples were subjected to different thermal treatments, as described below.

Catalyst Characterization. The chemical analysis of samples was performed with inductively coupled plasma atom emission spectroscopy at the CNRS Centre of Chemical Analysis (Vernaison, France).

Powder X-ray diffractograms (XRD) of samples as prepared were recorded at ambient atmosphere on a Siemens D5000 using the Cu Kα radiation ($\lambda = 154.05$ pm).

Transmission FT-IR spectra of self-supported Cr_xSiBEA wafers were recorded at room temperature on a Perkin-Elmer Spectrum One spectrometer (resolution of 2 cm^{-1}) after calcination at 773 K for 3 h in flowing air, followed by outgassing to 10^{-3} Pa at 573 K. Those wafers were contacted with gaseous pyridine via a separate cell containing liquid pyridine. Physisorbed pyridine was outgassed to 10^{-3} Pa at 423, 473, 523, and 573 K.

Diffuse reflectance (DR) UV−vis spectra of Cr_xSiBEA, either as prepared or after calcination at 773 K for 3 h in flowing air, followed by outgassing to 10^{-3} Pa at 773 K, were recorded at room temperature on a Cary 5E spectrometer equipped with an integrator and a double monochromator.

Temperature-programmed reduction (TPR) patterns were recorded on a Quantachrome Chembet 3000 apparatus. A 0.1 g sample was heated from 423 to 1123 K (10 K/min) in a flow of 5% H_2 in Ar. The H_2 consumption was monitored by a thermal conductivity detector (TCD). Prior to TPR, the samples were treated at 433 or 733 K in a flowing O_2/He mixture for 3 h. TPR patterns were fitted with a Gaussian function to determine the number of components under each peak.

X-ray photoelectron (XP) spectra were recorded on a spectrometer equipped with a hemispherical analyzer (SES R4000, Gammadata Scienta) using Al Kα (1486.6 eV) or Mg Kα (1253.6 eV) radiation. The power of the X-ray source was 300 W, and the energy pass for the analyzer was 100 eV, corresponding to a full width at half-maximum of 0.9 eV for the Ag $3d_{5/2}$ peak. The area of the sample analyzed was ∼3 mm^2. The powder samples were pressed on an indium foil and mounted on a special holder. Binding energy (BE) for Si, O, and Cr was measured by reference to the C 1s peak at 285.0 eV. XP spectra were recorded on Cr_xSiBEA either as prepared or calcined (773 K, 3 h, flowing air), then conditioned in dry air at 453 K and finally outgassed at room temperature to 10^{-7} Pa. All spectra were fitted with a Voigt function (a 70/30 composition of Gaussian and Lorentzian functions) to determine the number of components under each peak.

EPR spectra of Cr_xSiBEA either as prepared or calcined (773 K, 3 h, flowing air) and then outgassed to 10^{-3} Pa at the same temperature were recorded at 77 K on a Bruker ESP 300 spectrometer at 9.3 GHz (X band) with a 100 kHz field modulation and a modulation amplitude of 10 Gauss.

Catalysis Experiments. Prior to catalytic measurements, the Cr_xSiBEA samples were pretreated in flowing helium at 723 K for 0.5 h and hereafter referred to as activated Cr_xSiBEA. The ODH of propane with air or N_2O as oxidant was performed in a continuous flow reactor in the 573−673 K range at atmospheric pressure, with a weight hourly space velocity of 4500 mL h^{-1} g_{cat}^{-1} and a contact time of 0.8 s. The reactant mixture was composed of propane, N_2O (air), and helium in a molar ratio of 1:1.5:12.5. The products were analyzed with an online GC CHROM 5 apparatus equipped with a TCD or a flame ionization detector (FID). For products separation, the columns packed with Porapak R and SP 2340 were used. Coke deposit was determined by means of elementary analysis of spent catalyst over VARIO EL III apparatus produced by Elementar Company (Germany).

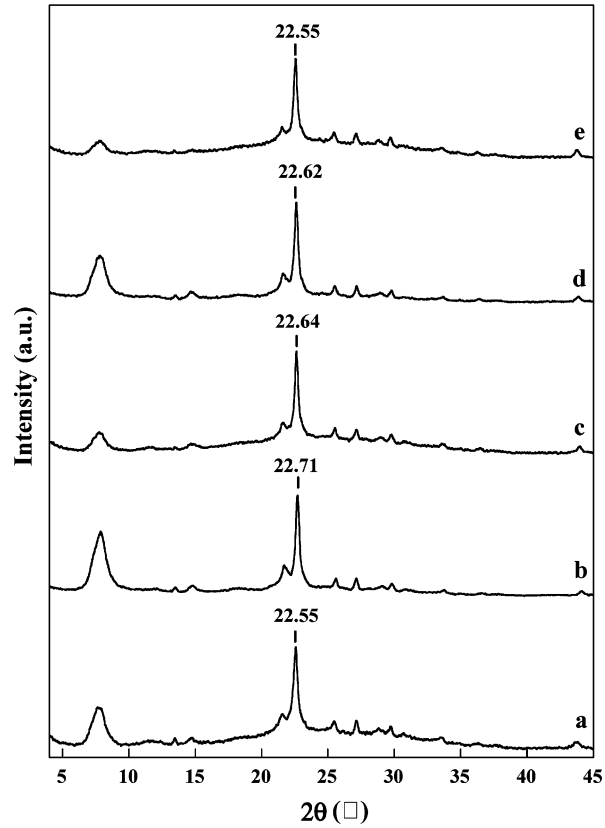

Figure 1. X-ray diffractograms of (a) AlBEA, (b) SiBEA, (c) $Cr_{0.2}$SiBEA, (d) $Cr_{1.0}$SiBEA, and (e) $Cr_{3.4}$SiBEA as prepared recorded at ambient atmosphere.

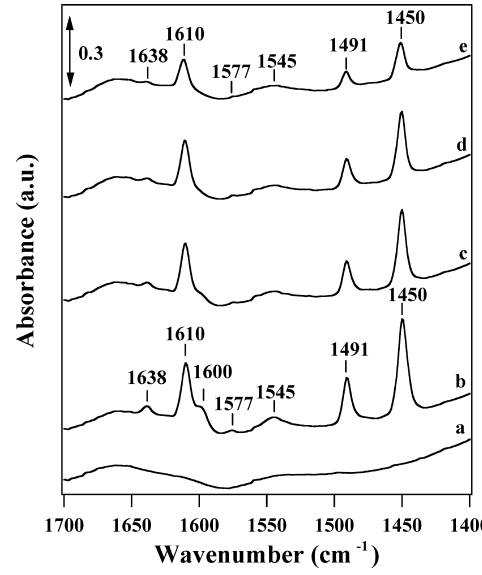

Figure 2. FTIR spectra of (a) $Cr_{3.4}$SiBEA after calcination at 773 K for 3 h in flowing air, followed by outgassing at 573 K to 10^{-3} Pa, and (b) adsorption of pyridine at room temperature, followed by outgassing at 423 K, (c) 473, (d) 523, and (e) 573 K to 10^{-3} Pa recorded at room temperature.

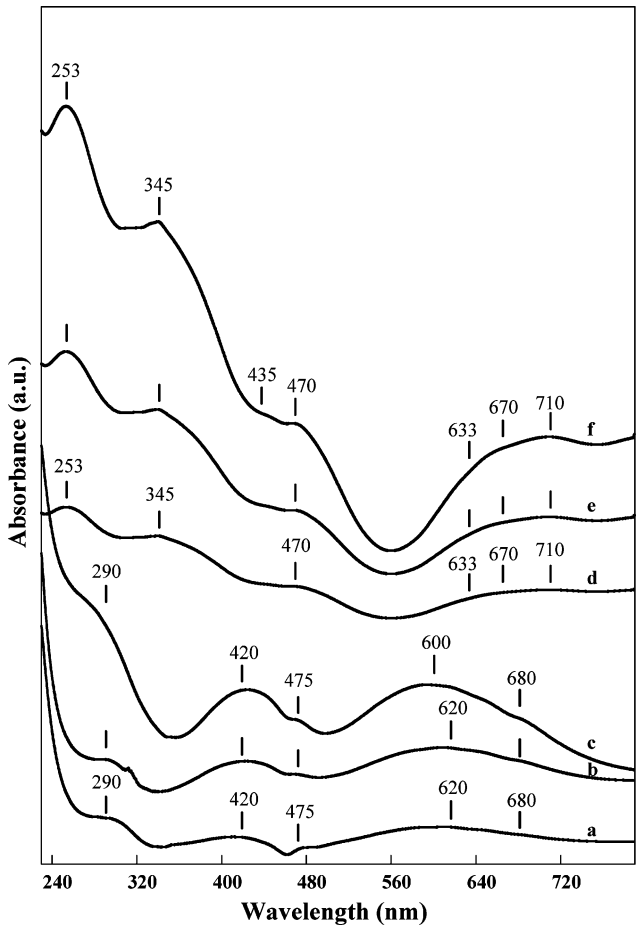

Figure 3. DR UV−vis spectra of (a) $Cr_{0.2}$SiBEA, (b) $Cr_{1.0}$SiBEA, and (c) $Cr_{3.4}$SiBEA as prepared and of (d) $Cr_{0.2}$SiBEA, (e) $Cr_{1.0}$SiBEA, and (f) $Cr_{3.4}$SiBEA after calcination at 773 K for 3 h in flowing air, followed by outgassing to 10^{-3} Pa at the same temperature recorded at ambient atmosphere.

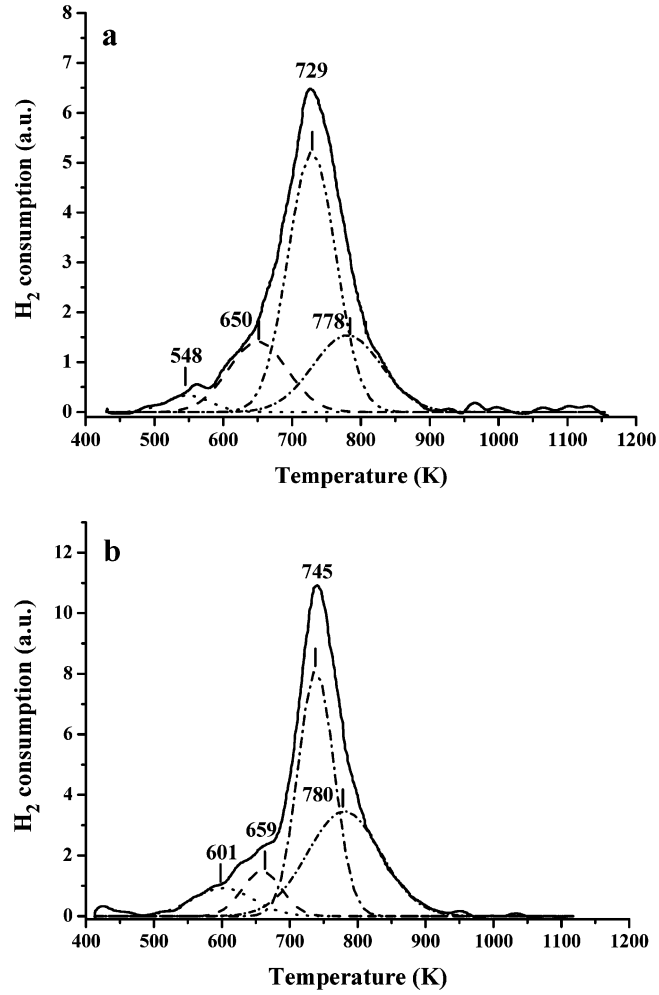

Figure 4. TPR patterns of (a) $Cr_{1.0}$SiBEA and (b) $Cr_{3.4}$SiBEA calcined at 773 K for 3 h in flowing air.

Results and Discussion

Nature of Chromium Species. ***X-ray Diffraction.*** Figure 1 shows the XRD patterns of AlBEA, SiBEA, $Cr_{0.2}$SiBEA, $Co_{1.0}$SiBEA, and $Co_{3.4}$SiBEA, which all are typical of the BEA zeolite, the crystallinity of which is not altered by dealumination. There is no evidence of extra-framework crystalline compounds or long-range amorphization of the zeolite. For BEA zeolite, a change of position of the narrow main diffraction peak around 22.60° is generally taken as evidence of framework contraction/expansion of the BEA zeolite.[34,35] The decrease of d_{302} spacing related to this peak from 3.942 (AlBEA; $2\theta = 22.55°$) to 3.912 Å (SiBEA; $2\theta = 22.71°$) upon dealumination indicates contraction of the matrix (Figure 1a and b). In contrast, the significant increase in d_{302} spacing from 3.912 Å (SiBEA; $2\theta = 22.71°$) to 3.939 ($Cr_{0.2}$SiBEA; $2\theta = 22.64°$), 3.940 ($Cr_{1.0}$SiBEA; $2\theta = 22.62°$), and 3.942 Å ($Cr_{3.4}$SiBEA; $2\theta = 22.55°$) (Figure 1c−e), after introduction of Cr ions into SiBEA, indicates some expansion of the BEA structure and suggests that the latter are probably incorporated into framework. It is important to mention here that the maximum number of framework vacant T-atoms sites in BEA zeolite is about 5.3 per unit cell, which is much higher than the number of Cr atoms per unit cell present in Cr_xSiBEA zeolites. This means that main amount of chromium could be introduced into framework sites of SiBEA zeolite.

FTIR Spectroscopy. The treatment of AlBEA zeolite by the HNO_3 solution suppresses the IR bands at 3781 and 3665 cm^{-1} attributed to AlO−H groups and at 3609 cm^{-1} attributed to Si−O(H)−Al groups, respectively (results not shown) as reported earlier.[27−29,36] The appearance of narrow bands at 3736 and 3710 cm^{-1} related to isolated SiO−H groups of SiBEA and of a broad band at 3520 cm^{-1} from H-bonded SiOH groups reveals the presence of vacant T-atom sites associated with SiO−H groups, as shown earlier.[27−29,36] The introduction of Cr leading to Cr_xSiBEA decreases the intensity of these bands, suggesting that SiO−H groups have reacted with chromium nitrate, as reported earlier by some of us.[36]

Figure 2 shows the FTIR spectra of $Cr_{3.4}$SiBEA after calcination at 773 K in air for 3 h, outgassing at 573 K (10^{-3} Pa) (Figure 2a), and adsorption of pyridine at room temperature and followed desorption at 423 (Figure 2b), 473 (Figure 2c), 523 (Figure 2d), and 573 K (Figure 2e). The bands typical of pyridinium cations are observed at 1545 and 1638 cm^{-1}, indicating the presence a small amount of Brønsted acidic sites. These data suggest that ≡Cr(III)−O(H)−Si≡ acidic sites are formed upon outgassing of $Cr_{3.4}$SiBEA, as suggested earlier for CrSiBEA.[36] Similar results were found for VSiBEA zeolite.[37]

The other bands at about 1610, 1600, 1577, 1491, and 1450 cm^{-1} observed (Figure 2b−e) correspond to pyridine interacting with Lewis acidic sites or pyridine physisorbed, which is in line with earlier data on CrSiBEA,[36] SiBEA, and VSiBEA.[38,39] Physisorbed pyridine (bands at 1600 and 1577 cm^{-1}) is removed by outgassing at temperature above 523 K. In contrast, pyridinium cations (bands at 1545 and 1638 cm^{-1}) and pyridine bonded to Lewis acidic sites (bands at 1610, 1491, and 1450

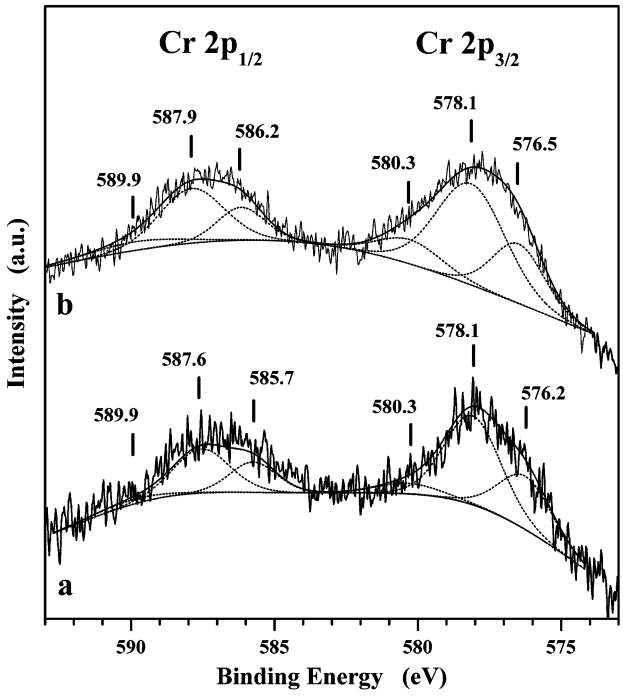

Figure 5. XP spectra of (a) $Cr_{1.0}$SiBEA as prepared and (b) $Cr_{1.0}$SiBEA calcined at 773 K for 3 h in flowing air.

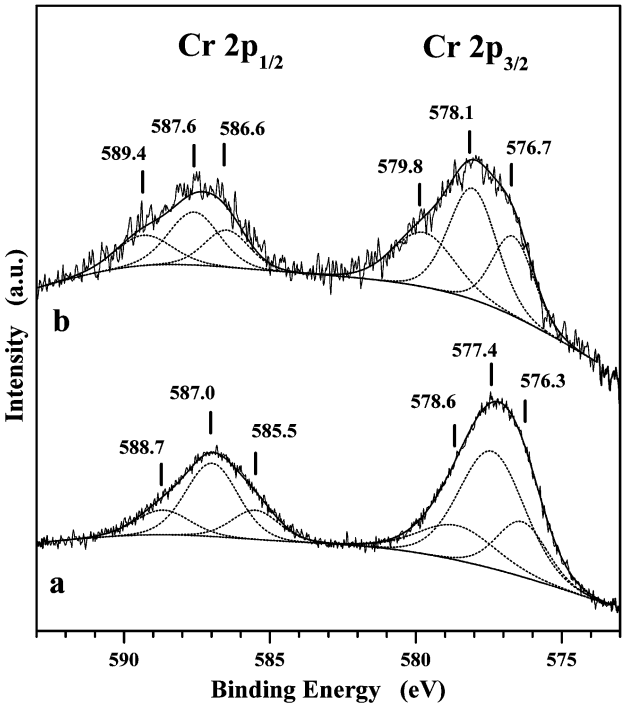

Figure 6. XP spectra of (a) $Cr_{3.4}$SiBEA as prepared and (b) $Cr_{3.4}$SiBEA calcined at 773 K for 3 h in flowing air.

cm^{-1}) remain even after outgassing at 573 K (Figure 2d−e), suggesting the presence in $Cr_{3.4}$SiBEA of strong Brønsted and Lewis acidic sites.

Diffuse Reflectance UV−vis Spectroscopy. Cr_xSiBEA as prepared exhibit three main bands at about 290, 420, and 600−620 nm (Figure 3). The two intense bands at 420 and 600−620 nm, the intensity of which increases with Cr content, are characteristic of octahedral Cr(III) and assigned to spin-allowed d−d transitions $^4A_{2g}(F) \rightarrow {}^4T_{1g}(F)$ and $^4A_{2g}(F) \rightarrow {}^4T_{2g}(F)$, respectively, in line with earlier work on CrSiBEA, Cr/Al_2O_3, and Cr-MCM-41[36,40−42] and consistent with the light

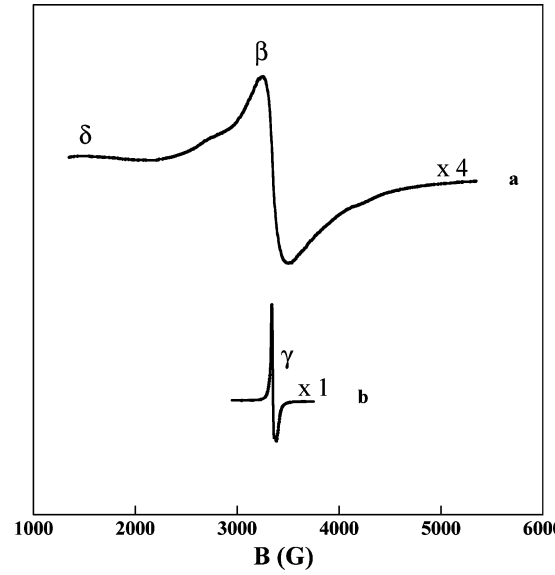

Figure 7. EPR spectra recorded at 77 K of (a) $Cr_{1.0}$SiBEA as prepared and (b) $Cr_{1.0}$SiBEA calcined at 773 K for 3 h in flowing air, followed by outgassing to 10^{-3} Pa at the same temperature.

green color of the samples, characteristic of octahedral Cr(III). The broad band at about 600−620 nm is asymmetric with a minor band at higher wavelength (∼680 nm), which is probably because of the spin-forbidden transition $^4A_{2g}(F) \rightarrow {}^2E_g$, $^2T_{1g}$ according to the Tanabe−Sugano diagram.[43] The band at 290 nm is characteristic of ligand to metal charge transfer (LMCT) transition involving octahedral Cr(III) ions. The band at about 475 nm, characteristic of LMCT transition of dichromate,[44−46] is weak suggesting that a very low amount of such species is present in Cr_xSiBEA as prepared.

Upon calcination at 773 K for 3 h in flowing air and further outgassing at 773 K to 10^{-3} Pa, two new intense bands appear at about 253 and 345 nm (Figure 3d−f), both ascribed to the $O^{2-} \rightarrow Cr^{6+}$ (d°) LMCT transition, suggesting that part of Cr(III) is oxidized to Cr(VI), in agreement with earlier data on Cr-containing aluminophosphate and silicoaluminophosphate and $Cr/SiO_2 \cdot Al_2O_3$.[47,48] Simultaneously, the color of Cr_xSiBEA changes from light-green to pale yellow. The almost complete disappearance of the main absorption bands of octahedral Cr(III) at 420 and 600−620 nm and the shoulder at 680 nm is in agreement with the oxidation of octahedral Cr(III) to tetrahedral Cr(VI). The increase in intensity of the band at about 470 nm, together with the appearance of the bands at 253 and 345 nm (Figure 4b), may indicate an increase in the amount of dichromate formed upon calcination, in agreement with earlier data on Cr-oxide-based catalysts[49] and Pt−Cr/ZSM-5.[50] Moreover, the broad band with submaxima at 633, 670, and 710 nm indicates also the presence of tetrahedral Cr(III) formed upon elimination of two water molecules, in agreement with earlier data on CrSiBEA,[36] Pt−Cr/ZSM-5,[51] and supported chromia catalysts.[52]

Temperature-Programmed Reduction. TPR experiments allow to correlate the reducibility of metal ions to their location and oxidation state, as reported earlier for Cr-containing zeolites, silicates, and oxides.[49−54]

The TPR patterns of $Cr_{1.0}$SiBEA and $Cr_{3.4}$SiBEA calcined in flowing air at 773 K for 3 h (Figure 4) can be deconvoluted into four components. The peaks at 729 and 778 K for $Cr_{1.0}$SiBEA and at 745 and 780 K for $Cr_{3.4}$SiBEA are probably the result of the reduction of isolated tetrahedral Cr(VI) and

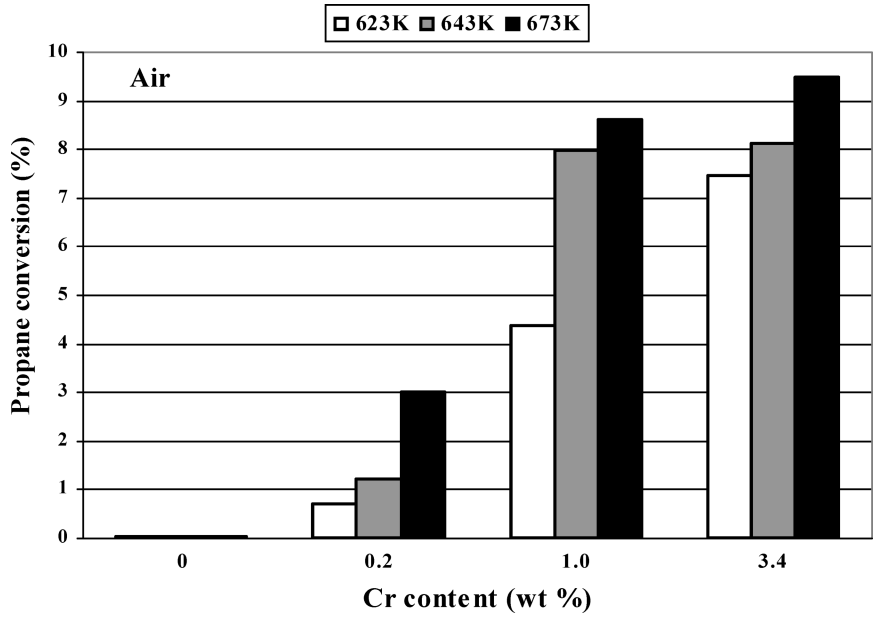

Figure 8. Propane conversion in ODH of propane with air as oxidant on activated SiBEA and Cr_xSiBEA measured at different reaction temperature as a function of Cr content.

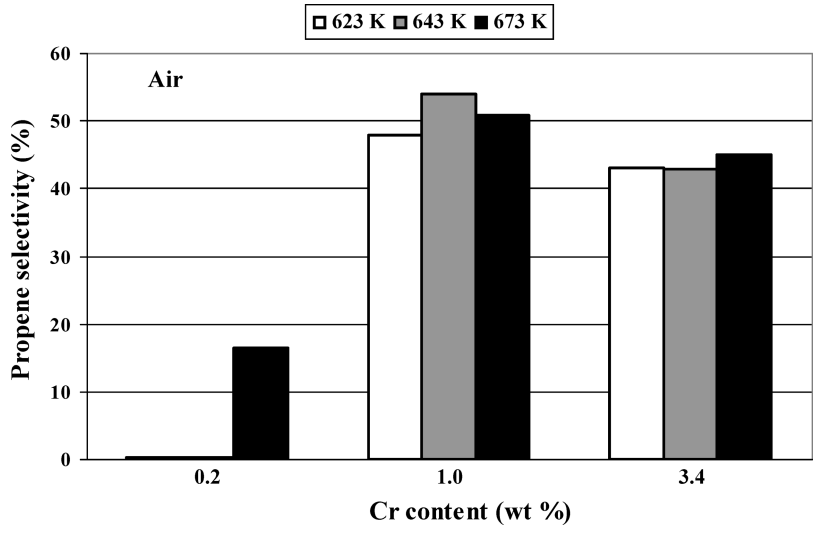

Figure 9. Selectivity toward propene in ODH of propane with air as oxidant on activated Cr_xSiBEA measured at different reaction temperature as a function of Cr content.

Cr(III) respectively, in line with earlier TPR and UV−vis data on Cr−HZSM-5, Cr/SiO_2, Cr/Al_2O_3[48] and Cr−MCM-41.[55]

The two peaks at 548 and 650 K for $Cr_{1.0}$SiBEA and 601 and 659 K for $Cr_{3.4}$SiBEA are probably caused by reduction of some extra-framework octahedral Cr(VI) (chromate or dichromate), expected to be reduced more easily than isolated tetrahedral Cr(VI) or Cr(III).

X-ray Photoelectron Spectroscopy. As shown in Figures 5 ($Cr_{1.0}$SiBEA as prepared and calcined) and 6 ($Cr_{3.4}$SiBEA as prepared and calcined), the peaks at about 578 and 587 eV corresponding to Cr $2p_{3/2}$ and Cr $2p_{1/2}$, respectively, can be deconvoluted into three components, hereafter referred to as low, intermediate, and high BE components. Following earlier reports on CrO_x/SiO_2,[56] Cr/clinoptilolite,[57] and Cr(VI) compounds,[58] the low BE component of Cr $2p_{3/2}$ at ∼ 576 eV and of Cr $2p_{1/2}$ at ∼ 586 eV (Figures 5 and 6) may correspond to tetrahedral Cr(III) ions, while the high BE component of Cr $2p_{3/2}$ at ∼ 580 eV and of Cr $2p_{1/2}$ at ∼ 589 eV may be attributed to octahedral Cr(VI).

The assignment of the most intense component, with intermediate BE, is more difficult. However, taking into account the UV−vis (Figure 3) and TPR data (Figure 4), we can assign it to isolated tetrahedral Cr(VI). Indeed, the disappearance of the main UV−vis bands of octahedral Cr(III) at 420 and 600−620 nm after calcination of Cr_xSiBEA (Figure 3) and the appearance of the bands at 253 and 345 nm (Figure 3d−f), both ascribed to the $O^{2-} \rightarrow Cr^{6+}$ (d°) LMCT transition, with simultaneous change of color of the samples from green to yellow, are consistent with the assignment, as well as the presence of the main TPR peak at 729−745 K for Cr_xSiBEA (Figure 4), because of the reduction of isolated tetrahedral Cr(VI) to Cr(III).

The component at high BE may be assigned to extra-framework octahedral Cr(VI). The intensity of this component suggests that the amount of extra-framework octahedral Cr(VI) is very low for $Cr_{1.0}$SiBEA (Figure 5) but significant for $Cr_{3.4}$SiBEA (Figure 6). These results are consistent with those of TPR presented in Figure 4 showing only a small amount of

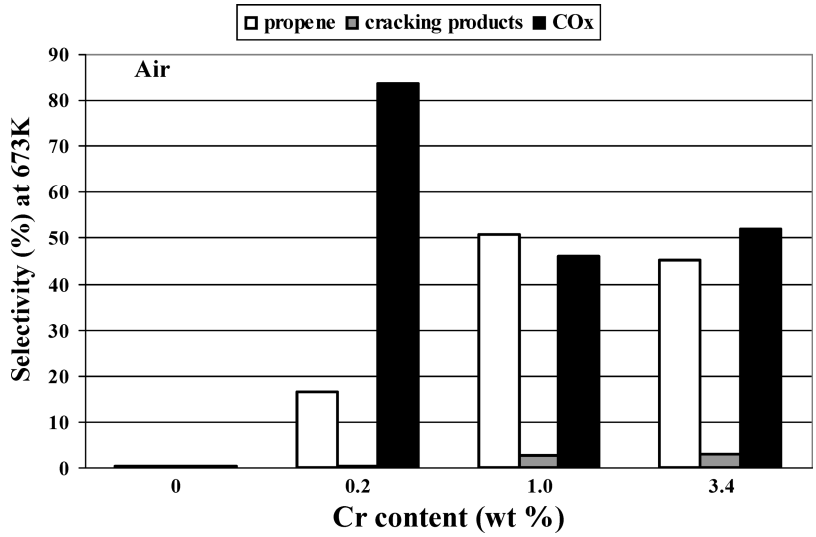

Figure 10. Selectivity toward different products (white, propene; gray, cracking products, ethene, methane; black, CO_x (CO, CO_2)) in ODH of propane with air as oxidant on activated Cr_xSiBEA measured at 673 K as a function of Cr content.

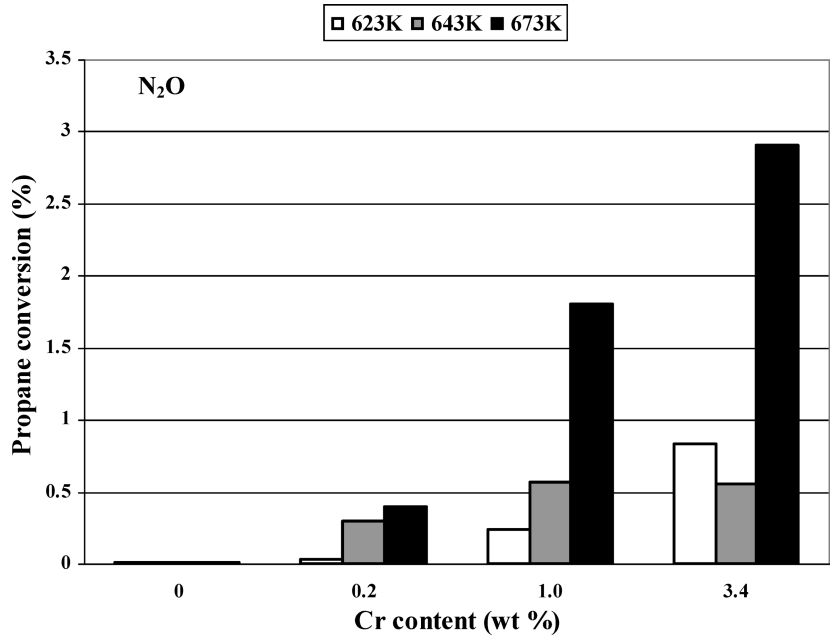

Figure 11. Propane conversion in ODH of propane with N_2O as oxidant on activated SiBEA and Cr_xSiBEA measured at different reaction temperature as a function of Cr content.

extra-framework octahedral Cr(VI) evidenced by the peaks at 540−650 K.

Moreover, taking into account the FTIR band at 1545 cm^{-1} (Figure 2) and its assignment, we can assign the component at low BE to isolated tetrahedral Cr(III) with a "Cr(III)−O(H)−Si" structure.

Electron Paramagnetic Resonance Spectroscopy. The signals denoted as β, γ, and δ generally found in the EPR spectra of Cr-supported materials[48,59] are also observed for Cr_xSiBEA. The EPR spectrum of $Cr_{1.0}$SiBEA as prepared recorded at 77 K (Figure 7a) is dominated by a broad isotropic signal at $g \approx 2$ (β signal) assigned to octahedral Cr(III).[48,59] The broad signal at $g \approx 5$ (δ signal), considered to be a fingerprint of isolated Cr(III) ions,[42] suggests that chromium in Cr_xSiBEA is mainly found as isolated octahedral Cr(III). The intense light-green color of these samples is consistent with this assignment.

The EPR spectrum of $Cr_{1.0}$SiBEA calcined (773 K, 3 h, flowing air) and then outgassed to 10^{-3} Pa at the same temperature shows a strong and sharp axial signal at $g = 1.972$ (γ signal) (Figure 7b), attributed to isolated Cr(V) species, as reported earlier for Cr−MCM-41, chromia/alumina, and Cr−silicalite-1.[42,60,61] This signal suggests that, upon calcination, followed by outgassing, part of Cr(III) is oxidized to Cr(V), consistent with the color change from light green to pale yellow. On the basis of DR UV−vis and EPR data, we can conclude that isolated octahedral Cr(III) is first oxidized upon calcination to isolated tetrahedral Cr(VI), while upon outgassing, some of them are reduced to isolated tetrahedral Cr(V) as indicated by the formation of the γ signal (Figure 7).

These observations underline the ability of Cr present in the framework of Cr_xSiBEA zeolite for changing its coordination and oxidation state.

Influence of Cr Content on the Catalytic Properties. ***Oxidative Dehydrogenation of Propane with Air.*** With air as oxidant, the conversion of propane on activated Cr_xSiBEA increases with Cr content and reaction temperature as shown

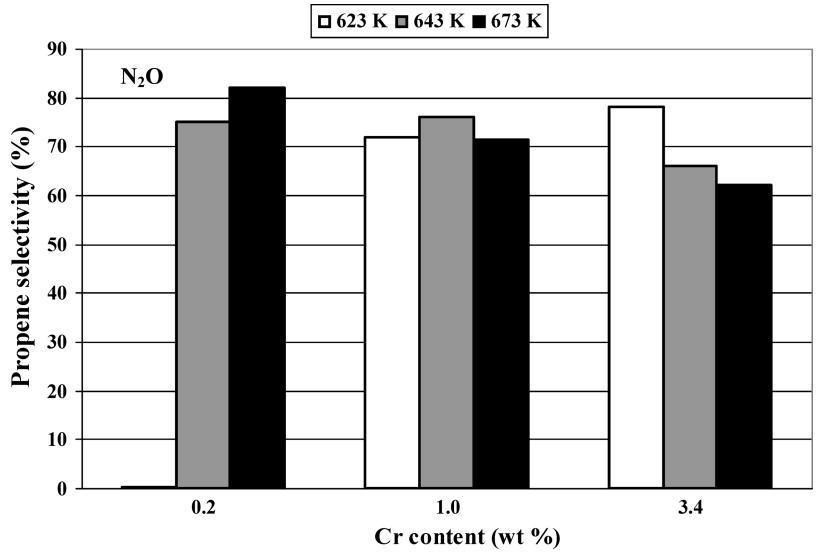

Figure 12. Selectivity toward propene in ODH of propane with N_2O as oxidant on activated Cr_xSiBEA measured at different reaction temperature as a function of Cr content.

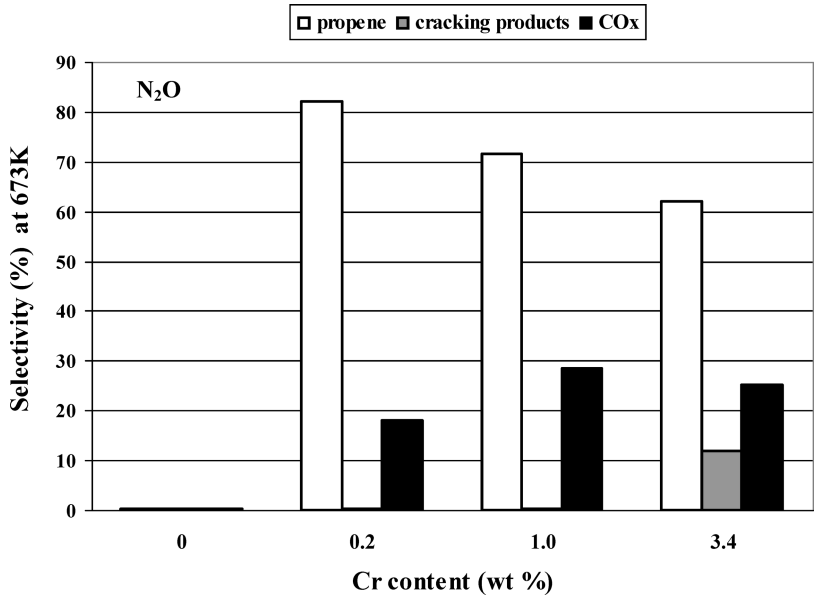

Figure 13. Selectivity toward different products (white, propene; gray, cracking products, ethene, methane; black, CO_x (CO, CO_2)) in ODH of propane with N_2O as oxidant on activated Cr_xSiBEA measured at 673 K as a function of Cr content.

in Figure 8. The selectivity toward propene lies in the range of 42−53% for Cr content of 1−3.4 wt % (Figure 9). Moreover, the selectivity toward cracking products (Figure 10), detected only above 623 K, does not exceed 5%. The selectivity toward CO_x (CO + CO_2), which lies above ∼50%, depends on the Cr content.

The sample with 0.2 Cr wt % shows a very low propane conversion (Figure 8) with CO_x as main product (Figure 10). Similar results were found for VSiBEA zeolite, which for very low content of V (0.1 wt %) mainly catalyzes total oxidation toward CO_2.[11,12] When the Cr content increases to 1.0 wt %, the selectivity toward propene increases to about 50%, while further increase to 3.4 wt % results in a small decrease.

Such change of activity and selectivity toward propene, observed in the whole temperature range (from 623 to 673 K) (Figure 9) confirms that ODH involves a particular type of Cr site, which amount changes with Cr content. On the basis of the characterization and catalysis results, it seems that the rather high selectivity toward propene for activated $Cr_{1.0}SiBEA$ and $Cr_{3.4}SiBEA$ is related to the presence of isolated tetrahedral Cr sites, while the slight decrease observed for $Cr_{3.4}SiBEA$ is probably related to the presence of extra-framework octahedral Cr sites, evidenced by UV−vis (Figure 3), TPR (Figure 4), and XPS (Figures 5, 6). These results are consistent with earlier data obtained for the ODH of propane on Fe-ZSM-5 zeolite[62] and showing that isolated tetrahedral Fe sites are responsible for the formation of propene and extra-framework FeO_x oligomers for the full oxidation.

Cracking products are formed in minor amount, suggesting that the number of strong Brønsted acidic sites is rather low. The latter are also responsible for the formation of a very small amount of coke (0.7 wt % after 5 h on stream), mainly observed at the reaction temperature of 673 K. The presence of coke does not influence the catalysts oxidative activity, suggesting that the sites promoting the ODH are not involved in the formation of coke. The carbon balance, which is satisfactory up to 5 h on stream, is close to 100%.

Oxidative Dehydrogenation of Propane with N_2O. With N_2O as oxidant, the conversion of propane on activated Cr_xSiBEA is much lower than in the presence of air (compare Figures 8 and 11) and increases with Cr content and reaction temperature. It appears that propane conversion on $Cr_{3.4}$SiBEA nearly attains 3% at 673 K showing that Cr_xSiBEA samples are not very active. In contrast, the selectivity toward propene lies between 60 and 80% in the 623−673 K range, except for $Cr_{0.2}$SiBEA, which does not produce propene below 643 K (Figure 12). The cracking products (mainly ethene with some amount of methane and only traces of ethane) appear on $Co_{3.4}$SiBEA only at 673 K (Figure 13).

The low propane conversion may originate from a very low concentration of isolated octahedral Cr(III) present in activated Cr_xSiBEA. It seems, that the presence of isolated tetrahedral Cr sites is essential for maintaining high selectivity toward propene, which is in line with earlier data on Cr on supported mesoporous MCM-41 silica.[63]

The amount of coke formation in the presence of N_2O (0.59 wt % of coke, after 5 h on stream) is about 15% lower than that observed in the presence of air. The coke appears mainly at the reaction temperature of 673 K, a result also observed for the ODH of propane with air. The carbon balance is close to 100% after 5 h of reaction.

Conclusions

Cr_xSiBEA samples (x = 0.2, 1.0, and 3.4 Cr wt %) are prepared by a two-step postsynthesis method. After removal of Al from BEA zeolite, the probable incorporation of Cr ions into the framework of the resulting SiBEA zeolite, evidenced by XRD, generates Brønsted acidic sites, such as ≡Cr(III)−O(H)−Si≡, as shown by FTIR of pyridine adsorbed as probe molecule.

DR UV−vis, TPR, and XPS data suggest that chromium is mainly present as isolated octahedral Cr(III) in Cr_xSiBEA as prepared and as isolated tetrahedral Cr(VI) in calcined Cr_xSiBEA. The amount of these species increases with Cr content. Upon outgassing at 773 K of the calcined sample, part of isolated tetrahedral Cr(VI) is reduced to isolated tetrahedral Cr(V), as shown by EPR. These observations underline the ability of Cr present in Cr_xSiBEA for changing its coordination.

The activity and selectivity of Cr_xSiBEA for the ODH of propane strongly depend on the coordination of chromium present in activated Cr_xSiBEA, as well as the type of oxidant. The presence of isolated tetrahedral Cr sites with oxidation state lower that (VI) on activated Cr_xSiBEA is essential for maintaining a high selectivity in the presence of air or N_2O.

In the presence of air, the propane conversion increases with Cr content, while the selectivity toward propene is highest for the sample with 1.0 wt % of Cr. The lower selectivity to propene on sample with 3.4 wt % of Cr is probably related to the presence of some amount of extra-framework octahedral Cr sites.

The propane conversion is lower in the presence of N_2O and reaches only ∼3% at 673 K for $Cr_{3.4}$SiBEA. In contrast, the selectivity to propene is higher in the presence of N_2O than of air. It is probably related to the degree of Cr reduction under reaction conditions and to the nature of surface oxygen formed in the presence of N_2O or air.

Acknowledgment. S.D. gratefully acknowledges the CNRS (France) for financing his research position and J.J. acknowledges the GDRI CNRS-PAN for financial support of his stay in Paris.

References and Notes

(1) Gao, X.; Bare, S. R.; Weckhuysen, B. M.; Wachs, I. E. *J. Phys. Chem. B* **1998**, *102*, 10842.
(2) Owens, L.; Kung, H. H. *J. Catal.* **1993**, *144*, 202.
(3) Klisińska, A.; Haras, A.; Samson, K.; Witko, M.; Grzybowska, B. *J. Mol. Catal. A* **2004**, *210*, 87.
(4) Centi, G.; Trifiro, F. *Appl. Catal., A* **1996**, *143*, 3.
(5) Lopez Nieto, J. M.; Kremenic, G.; Fierro, J. L. G. *Appl. Catal.* **1990**, *61*, 235.
(6) Albonetti, S.; Cavani, F.; Trifiro, F. *Catal. Rev. Sc. Eng.* **1996**, *38*, 413.
(7) Blasco, T.; Concepcion, P.; Lopez Nieto, J. M.; Perez-Pariente, J. *J. Catal.* **1995**, *152*, 1.
(8) Santamaría-González, J.; Luque-Zambrana, J.; Mérida-Robles, J.; Maireles-Torres, P.; Rodríguez-Castellón, E.; Jiménez-López, A. *Catal. Lett.* **2000**, *68*, 67.
(9) Sulikowski, B.; Olejniczak, Z.; Włoch, E.; Rakoczy, J.; Valenzuela, R. X.; Cortés Corberán, V. *Appl. Catal., A* **2002**, *232*, 189.
(10) Kartheuser, B.; Hodnett, B. K. *J. Chem. Soc., Chem. Commun.* **1993**, 1093.
(11) Dzwigaj, S.; Gressel, I.; Grzybowska, B.; Samson, K. *Catal. Today* **2006**, *114*, 237.
(12) Dzwigaj, S.; Che, M.; Grzybowska, B.; Gressel, I.; Samson, K. *Stud. Surf. Sci. Catal.* **2007**, *172*, 385.
(13) Khodakov, A.; Olthof, B.; Bell, A. T.; Iglesia, E. *J. Catal.* **1999**, *181*, 205.
(14) Blasco, T.; Lopez Nieto, J. M. *Appl. Catal., A* **1997**, *157*, 117.
(15) Cavani, F.; Koutyrev, M.; Trifiro, F.; Bartolini, A.; Ghisletti, D.; Iezzi, R.; Santucci, A.; Piero, G. *J. Catal.* **1996**, *158*, 236.
(16) Jiménes-López, A.; Rodriguez-Castellón, E.; Maireles-Torres, P.; Diaz, L.; Mérida-Robles, J. *Appl. Catal., A* **2001**, *218*, 295.
(17) Cavani, F.; Trifiro, F. *Catal. Today* **1995**, *24*, 307.
(18) Held, A.; Kowalska, J.; Nowinska, K. *Appl. Catal., B* **2006**, *64*, 201.
(19) Pérez-Ramírez, J.; Gallardo-Llamas, A. *J. Catal.* **2004**, *223*, 382.
(20) Novoveská, K.; Bulánek, R.; Wichterlova, B. *Catal. Today* **2005**, *100*, 315.
(21) Reddy, J. S.; Sayari, A. *J. Chem. Soc., Chem. Commun.* **1995**, 23.
(22) Thangaraj, A.; Sivasanker, S.; Ratnasamy, P. *J. Catal.* **1991**, *131*, 394.
(23) Kraushaar, B.; van Hooff, J. H. C. *Catal. Lett.* **1989**, *2*, 43.
(24) Yamashita, H.; Yoshizawa, K.; Ariyuki, M.; Highashimoto, S.; Che, M.; Anpo, M. *J. Chem. Soc., Chem. Commun.* **2001**, 435.
(25) Raghavan, P. S.; Ramaswamy, V.; Upadhya, T. T.; Sudalai, A.; Ramaswamy, A. V.; Sivasanker, S. *J. Mol. Catal.* **1997**, *122*, 75.
(26) Dai, P. S. E.; Lunsford, J. H. *J. Catal.* **1980**, *64*, 173.
(27) Dzwigaj, S.; Peltre, M. J.; Massiani, P.; Davidson, A.; Che, M.; Sen, T.; Sivasanker, S. *J. Chem. Soc., Chem. Commun.* **1998**, 87.
(28) Dzwigaj, S.; Matsuoka, M.; Franck, R.; Anpo, M.; Che, M. *J. Phys. Chem. B* **1998**, *102*, 6309.
(29) Dzwigaj, S.; Matsuoka, M.; Anpo, M.; Che, M. *J. Phys. Chem. B* **2000**, *104*, 6012.
(30) Dzwigaj, S.; Che, M. *J. Phys. Chem. B* **2006**, *110*, 12490.
(31) Janas, J.; Machej, T.; Gurgul, J.; Socha, L. P.; Che, M.; Dzwigaj, S. *Appl. Catal., B* **2007**, *75*, 239.
(32) Dzwigaj, S.; Janas, J.; Machej, T.; Che, M. *Catal. Today* **2007**, *119*, 133.
(33) Dzwigaj, S.; Stievano, L.; Wagner, F. E.; Che, M. *J. Phys. Chem. Solids* **2007**, *68*, 1885.
(34) Camblor, M. A.; Corma, A.; Perez-Pariente, J. *Zeolites* **1993**, *13*, 82.
(35) Reddy, E. P.; Davydov, L.; Smirniotis, G. *J. Phys. Chem. B* **2002**, *106*, 3394.
(36) Dzwigaj, S.; Shishido, T. *J. Phys. Chem. C* **2008**, *112*, 5803.
(37) Dzwigaj, S.; El Malki, E. M.; Peltre, M. J.; Massiani, P.; Davidson, A.; Che, M. *Top. Catal.* **2000**, *11/12*, 379.
(38) Dzwigaj, S.; Massiani, P.; Davidson, A.; Che, M. *J. Mol. Catal. A* **2000**, *155*, 169.
(39) Gora-Marek, K.; Datka, J.; Dzwigaj, S.; Che, M. *J. Phys. Chem. B* **2006**, *110*, 6763.
(40) Weckhuysen, B. M.; Schoonheydt, R. A. *Catal. Today* **1999**, *51*, 223.
(41) Zhu, Z.; Chang, Z.; Kevan, L. *J. Phys. Chem. B* **1999**, *103*, 2680.
(42) Lezanska, M.; Szymanski, G. S.; Pietrzyk, P.; Sojka, Z.; Lercher, J. A. *J. Phys. Chem. C* **2007**, *111*, 1930.
(43) Tanabe, Y.; Sugano, S. *J. Phys. Soc. Jpn.* **1954**, *9*, 753.
(44) Ohshiro, S.; Chiyoda, O.; Maekawa, K.; Masui, Y.; Anpo, M.; Yamashita, H. C. R. *Chimie* **2006**, *9*, 846.
(45) Wang, Y.; Ohoshi, Y.; Shishido, T.; Zdang, Q.; Yang, W.; Guo, Q.; Wan, H.; Takehira, K. *J. Catal.* **2003**, *220*, 347.
(46) Takehira, K.; Ohoshi, Y.; Shishido, T.; Kawabata, T.; Takaki, K.; Zhang, Q.; Wang, Y. *J. Catal.* **2004**, *224*, 404.

(47) Hartmann, M.; Kevan, L. *Chem. Rev.* **1999**, *99*, 635.
(48) Weckhuysen, B. M.; Schoonheydt, R. A.; Jehna, J.; Wachs, I. E.; Cho, S. J.; Ryoo, R.; Kijlstra, S.; Poels, E. *J. Chem. Soc., Faraday Trans* **1995**, *91*, 3245.
(49) Al-Zahrani, S. M.; Jibril, B. Y.; Abasaeed, A. E. *Catal. Today* **2003**, *81*, 507.
(50) Raddi de Araujo, L. R.; Schmal, M. *Appl. Catal., A* **2002**, *235*, 139.
(51) Cherian, M.; Rao, M. S.; Hirt, A. M.; Wachs, I. E.; Deo, G. *J. Catal.* **2002**, *211*, 482.
(52) Liotto, L. F.; Venezia, A. M.; Pantaleo, G.; Deganello, G.; Gruttaduria, M.; Noto, R. *Catal. Today* **2004**, *91*−*92*, 231.
(53) Wichterlova, B.; Tvarůzkova, Z.; Novakova J., *J. Chem. Soc., Faraday Trans. I* **1983**, *79*, 1583.
(54) Zhang, Y.; Matos, I.; Lemos, M. A. N. D. A.; Freire, F.; Nunes, T. G.; Botelho do Rego, A. M.; Henriques, R. T.; Fonseca, I. F.; Marques, M. M.; Lemos, F. *J. Polym. Sci., Part A* **2003**, *41*, 3768.
(55) Zhu, Z.; Hartmann, M.; Maes, E. M.; Czernuszewicz, R. S.; Kevan, L. *J. Phys. Chem. B* **2000**, *104*, 4690.
(56) Liu, B.; Terano, M. *J. Mol. Catal. A* **2001**, *172*, 227.
(57) Logar, N. Z.; Siljeg, M.; Arcon, I.; Meden, A.; Tusar, N. N.; Stefanovic, S. C.; Kovac, J.; Kaucic, V. *Microporous Mesoporous Mater.* **2006**, *93*, 275.
(58) Gili, P.; Lorenzo-Luis, P. A. *Coord. Chem. Rev.* **1999**, *193*−*195*, 747.
(59) Mimura, N.; Okamoto, M.; Yamashita, H.; Oyama, S. T.; Murata, K. *J. Phys. Chem. B* **2006**, *110*, 21764.
(60) Puurunen, R. L.; Weckhuysen, B. M. *J. Catal.* **2002**, *210*, 418.
(61) Chapus, T.; Tuel, A.; Ben Taarit, Y.; Naccache, C. *Zeolites* **1994**, *14*, 349.
(62) Perez-Ramirez, J.; Gallardo-Llamas, A. *Appl. Catal., A* **2005**, *279*, 117.
(63) Santamaría-González, J.; Mérida-Robles, J.; Alcantara-Rodriguez, M.; Maireles-Torres, P.; Rodríguez-Castellón, E.; Jiménez-López, A. *Catal. Lett.* **2000**, *64*, 209.

JP809733S